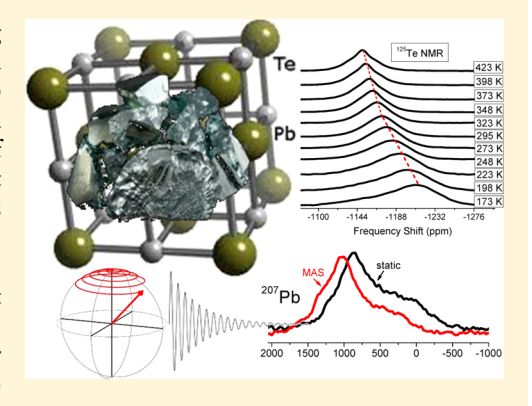
# A Combined NMR and DFT Study of Narrow Gap Semiconductors: The Case of PbTe

Robert E. Taylor, † Fahri Alkan, † Dimitrios Koumoulis, † Michael P. Lake, † Daniel King, † Cecil Dybowski, † and Louis-S. Bouchard\*,†,§

Supporting Information

ABSTRACT: In this study we present an alternative approach to separating contributions to the NMR shift originating from the Knight shift and chemical shielding by a combination of experimental solid-state NMR results and ab initio calculations. The chemical and Knight shifts are normally distinguished through detailed studies of the resonance frequency as a function of temperature and carrier concentration, followed by extrapolation of the shift to zero carrier concentration. This approach is time-consuming and requires studies of multiple samples. Here, we analyzed <sup>207</sup>Pb and <sup>125</sup>Te NMR spinlattice relaxation rates and NMR shifts for bulk and nanoscale PbTe. The shifts are compared with calculations of the <sup>207</sup>Pb and <sup>125</sup>Te chemical shift resonances to determine the chemical shift at zero charge carrier concentration. The results are in good agreement with literature values from carrier concentration-dependent studies. The measurements are also compared to literature reports of the <sup>207</sup>Pb and <sup>125</sup>Te Knight shifts of *n*- and *p*-type PbTe



semiconductors. The literature data have been converted to the currently accepted shift scale. We also provide possible evidence for the "self-cleaning effect" property of PbTe nanocrystals whereby defects are removed from the core of the particles while preserving the crystal structure.

## ■ INTRODUCTION

Lead telluride is a narrow gap semiconductor long used for thermoelectric applications. Snyder and co-workers<sup>1</sup> recently provided an overview of the scientific and technological history of this material. The overview begins "during the Cold War and Space Race of the middle part of the 20th century" and concludes by discussing how band structure engineering to improve overall thermoelectric efficiency has recently been driving this field of research. Among the many ways to interrogate the state of semiconductors such as PbTe, nuclear magnetic resonance (NMR) of both nuclei has been extremely valuable in assessing the electronic state.<sup>2-7</sup> For example, the Knight shift,8 which probes the interaction of nuclear spins with conduction band carriers (electrons or holes), provided a direct measure of carrier concentration. This readout can be performed even on samples that are not amenable to transport studies. Such readouts could, in principle, aid in the development of novel materials which cannot be produced as high quality thin films or single crystals. This potentially important technological application is currently hampered, however, by our inability to separate Knight shift from chemical

The Knight shift is typically measured relative to the resonance of the nucleus of interest in a "carrier-free sample",

hence the importance of the reference point. Nuclei such as <sup>207</sup>Pb experience strong chemical shielding contributions to the overall shift. These early studies report the Knight shifts as the magnetic field for the resonance of <sup>207</sup>Pb and <sup>125</sup>Te nuclei at a given radio frequency (RF). In these terms, the Knight shift, K, is given by<sup>6</sup>

$$K = (H_r - H_s)/H_s \tag{1}$$

where  $H_r$  is the magnetic field at which the resonance of a sample free of charge carriers occurs, i.e., a sample whose resonance is governed only by the chemical shielding.  $^{9,10}$   $H_{\rm s}$  is the resonance field of a "real sample [...] at constant frequency". The chemical-shielding reference field,  $H_r$ , is usually determined indirectly by extrapolating the dependence of  $H_s$  on carrier concentration (measured by some other technique) back to zero carrier concentration.

There are some challenges in determining the chemical shielding and expressing magnetic field values reported in the earlier literature in terms of the current convention for chemical shifts 11

Received: October 15, 2012 Revised: April 6, 2013 Published: April 10, 2013

Department of Chemistry and Biochemistry, University of California, Los Angeles, California 90095-1569, United States

<sup>&</sup>lt;sup>‡</sup>Department of Chemistry and Biochemistry, University of Delaware, Newark, Delaware 19761-2522, United States

<sup>§</sup>California NanoSystems Institute, UCLA, Los Angeles, California 90095-1569, United States

$$\delta(\text{ppm}) = \left\{ \frac{(\nu_{\text{sample}} - \nu_{\text{reference}})}{\nu_{\text{reference}}} \right\} \times 10^6$$
 (2)

One challenge is the accuracy with which the resonance field can be read from graphs in the older literature. Another issue arises from the temperature dependence of the chemical shifts and Knight shifts. The chemical shifts of diamagnetic lead compounds often have a strong dependence on temperature. As an example, the <sup>207</sup>Pb resonance of lead nitrate is routinely used as a NMR thermometer because of the 0.76 ppm/K change of the resonance position with temperature. <sup>12–19</sup> Separating the temperature dependence of the Knight shift from that of the chemical shift can be done only for temperature studies with different samples of *n*- and *p*-type semiconductors. This procedure is time-consuming and strongly depends on the quality of the samples and their characterization by transport measurements. The reliability of transport measurements in turn depends on sample quality.

Previous experiments focused on <sup>207</sup>Pb and <sup>125</sup>Te NMR line positions as functions of carrier concentration and temperature; band structure calculations provided a qualitative understanding of the results and energy gap. The <sup>207</sup>Pb and <sup>125</sup>Te chemical shifts relative to the resonance of a standard material are dependent on the local structure and electronic environment. As a result, chemical shift tensors provide qualitative trends that yield insights into the chemical bonding. The structure of PbTe is particularly simple, which allows one to compare experimentally measured chemical shifts with first-principles calculations.

The nuclear magnetic relaxation of <sup>207</sup>Pb and <sup>125</sup>Te reflects the dynamics of fluctuating magnetic fields in the vicinity of the nucleus. In semiconductors, relaxation is frequently dominated by spin-flip scattering with the conduction charge carriers. As such, the relaxation behavior is correlated with the Knight shift. The relaxation behavior of both <sup>207</sup>Pb and <sup>125</sup>Te as a function of temperature confirms, as with the shifts, that the sample contains a distribution of electronic environments.<sup>20</sup>

# ■ EXPERIMENTAL AND THEORETICAL METHODS

The NMR data were acquired with a Bruker DSX-300 spectrometer operating at a frequency of 62.79 MHz for <sup>207</sup>Pb and 94.69 MHz for <sup>125</sup>Te. A standard Bruker X-nucleus wide-line probe with a 5-mm solenoid coil was used with a static polycrystalline sample of PbTe. The PbTe samples were obtained from Sigma Aldrich (avg. size: 84% smaller than 177  $\mu$ m and 13% between 177 and 354  $\mu$ m) and Alfa Aesar. The PbTe particle size was small enough to avoid RF skin-depth effects at these frequencies. The sample was confined to the length of the RF coil. The  $^{207}$ Pb  $\pi/2$  pulse width was 4.5  $\mu$ s, and the  $^{125}\text{Te}~\pi/2$  pulse width was 4  $\mu$ s. We have verified that these RF pulses excited the entire NMR resonances. Magicangle spinning (MAS)<sup>21–23</sup> spectra were acquired on the same sample with a standard Bruker MAS probe using a 4-mm outside diameter zirconia rotor with a sample spinning rate of 10 kHz. The  $^{207}$ Pb and  $^{125}$ Te  $\pi/2$  pulse widths for the MAS experiments were 4.4  $\mu$ s. To minimize pulse ringdown effects, spectral data were acquired using a spin-echo sequence  $[\pi/2]_x$  $(\tau - \tau - \pi)_{\nu}$  -  $\tau$  - acquire] with the echo delay,  $\tau$ , set to 20  $\mu$ s. Data for determining the spin-lattice relaxation times  $(T_1)$  were acquired with a saturation-recovery technique.<sup>24</sup> The <sup>207</sup>Pb and  $^{125}\mathrm{Te}$  chemical shift scales were calibrated using the unified  $\Xi$ scale, 11 relating the nuclear resonance frequency to the 1H

resonance of dilute tetramethylsilane in CDCl<sub>3</sub> at a frequency of 300.13 MHz. The reference for  $^{207}\mathrm{Pb}$  is tetramethyllead (TML) and the reference for  $^{125}\mathrm{Te}$  is dimethyltelluride. The two chemical shift scales were experimentally verified by acquiring spectra of lead nitrate  $^{16-18}$  and telluric acid. We also note the existence of alternative  $^{125}\mathrm{Te}$  absolute chemical shielding scales and comparisons to density functional theory (DFT) predictions.  $^{26-28}$  A relaxation delay of at least five times  $T_1$  was used in each experiment to allow full recovery of the magnetization.

Quantum calculations were performed with the Amsterdam Density Functional theory (ADF) suite of software<sup>29–31</sup> on models of the local PbTe environment. Calculations employed the Becke88–Perdew86 generalized gradient approximation (BP86) functional<sup>32,33</sup> and a triple-ζ double polarized (TZ2P) basis set. The calculations included relativistic effects by the zero order regular approximation (ZORA) to the two-component Dirac equation with spin–orbit coupling.<sup>34,35</sup> NMR chemical shieldings were calculated with the NMR module<sup>36</sup> associated with the ADF program package. The <sup>207</sup>Pb chemical shifts are reported relative to TML, whose isotropic chemical shift was calculated at the same level of theory. The <sup>125</sup>Te chemical shifts are reported relative to dimethyltelluride.

## ■ RESULTS AND DISCUSSION

**Chemical Shifts.** With modern NMR spectrometers, the <sup>207</sup>Pb resonance frequency is typically measured in a magnetic field of a fixed strength. The measured NMR shift includes contributions from chemical shielding and the Knight shift. For diamagnetic insulators, the chemical shift of <sup>207</sup>Pb can range up to 12 000 ppm relative to TML.<sup>37</sup> Similarly, the range of chemical shifts of <sup>125</sup>Te is approximately 5000 ppm. The <sup>207</sup>Pb Knight shifts are among the largest known shifts for nontransition materials, on the order of 1% for a carrier concentration of 10<sup>19</sup> cm<sup>-3</sup> in *n*- and *p*-type PbTe semiconductors<sup>5</sup> (although the <sup>125</sup>Te shift remains small in these materials). As mentioned previously, the contributions of the two components to the overall shift can be separated because the Knight shift is experimentally determined by measuring the resonance position relative to that of a "carrier-free sample".<sup>3</sup>

Lead telluride has been investigated with temperature-dependent NMR spectroscopy by several groups. <sup>2-7</sup> The theoretical challenge has been to explain the large Knight shift of <sup>207</sup>Pb arising from both the *s*-like holes and *p*-like conduction electrons. As discussed by Sapoval and co-workers, <sup>4,5</sup> the early theory suggested that only *s*-like electrons give rise to a large Knight shift. They noted that more comprehensive models with the full expression for hyperfine coupling indicated that large Knight shifts can also arise from the spin—orbit term for *p*-type electrons and that a dipolar field from the electron, "even in cubic crystals", <sup>5</sup> can arise due to the spin—orbit term.

These early studies typically reported Knight shifts as the magnetic field for the resonance of <sup>207</sup>Pb nuclei at a given RF according to eq 1. These experiments were done in the swept-field/constant frequency mode. The resonance fields of <sup>207</sup>Pb at a frequency of 7.5056 MHz as a function of the carrier concentration for a series of *n*- and *p*-type PbTe at 1.3 K have been measured and extrapolated back to a field of 8436 gauss for a hypothetical sample of zero carriers<sup>2,5</sup> to yield the chemical shift of PbTe at that temperature. A different study<sup>3</sup> reported the resonance fields of <sup>207</sup>Pb at a frequency of 10.0 MHz as a function of the carrier concentration for a series of *n*-

and *p*-type PbTe samples from 77 to 465 K. This work indicated a field of 11 216 gauss as the zero-charge-carrier resonance field at 300 K. The combination of these two studies provides the temperature dependence of the chemical shift of PbTe.

As the resonance frequency is directly proportional to the magnetic field, the observed resonance frequency can be scaled to a different magnetic field. This process was used in many early studies for comparison of experimental results. To express these experimental results from earlier studies in terms of current conventions<sup>11</sup> and to compare them directly with the experimental results reported in the present work, we have converted these earlier results to the appropriate frequencies that would be observed in a magnetic field of 7.04925 T in which the protons of tetramethylsilane are observed at a frequency of 300.130 MHz. These frequencies at 7.04925 T were then converted to parts per million (ppm) relative to the reference material by use of eq 2 and the unified  $\Xi$  scale as described in ref 11. (Examples of this conversion process are explicitly shown in the Supporting Information.) Sapoval's extrapolation<sup>4</sup> for the <sup>207</sup>Pb chemical shift of PbTe at 1.3 K can be expressed as -420.8 ppm. The variable-temperature study<sup>3</sup> yields a <sup>207</sup>Pb chemical shift of 970.8 ppm at 300 K.

The <sup>207</sup>Pb spectrum of a static polycrystalline sample of PbTe at 295 K is shown in Figure 1a. The resonance line shape is

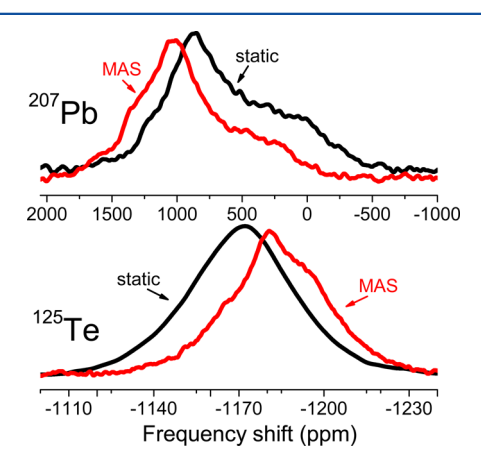


**Figure 1.** (a)  $^{207}$ Pb spectrum (black line) of static polycrystalline PbTe at 295 K. The  $^{207}$ Pb MAS spectrum is shown below (red line). (b)  $^{125}$ Te spectrum (black line) of static polycrystalline PbTe at 295 K. The  $^{125}$ Te MAS spectrum is shown below (red line).

clearly asymmetric. Such an asymmetrical feature likely arises from interaction with conduction carriers.  $^{38-47}$  In a prior study,  $^{48,49}$  asymmetric resonance lines were attributed to an inhomogeneous distribution of defects yielding different charge carrier concentrations in different microcrystalline regions, giving a range of Knight shifts for spins in these different environments. Specifically, the  $^{207}$ Pb Knight shift in the case of PbTe with low p-type carrier concentrations has been reported to go as  $n^{1/3}$ , where n is the charge carrier concentration. The tensorial nature of the electron—nuclear hyperfine interaction, namely, the contributions from dipolar and orbital terms in a material with p-band charge carriers, could also contribute to the asymmetry of the line shape.  $^{50}$ 

In the  $^{207}\text{Pb}$  spectrum of the static sample shown in Figure 1a, the experimental resonance extends from roughly 1600 ppm to about -500 ppm, with a maximum intensity at ca. 875 ppm. In Figure 1a, the spectrum of the sample obtained under MAS

has essentially the same structure, but it is slightly shifted to higher frequencies, with the maximum intensity at  $\sim\!1000$  ppm. If the least shielded areas of the sample correspond to lower carrier concentrations, the results of Figure 1a suggest a chemical shift at 295 K of between 1200 and 1400 ppm. For comparison with the earlier literature (as converted for the present work), Sapoval and co-workers report a chemical shift of -420.8 ppm at a temperature of 1.3 K. The later work by Senturia, et al. gives a chemical shift of 970.8 ppm at 300 K. From these observations, we conclude that the  $^{207}\text{Pb}$  chemical shift of PbTe is in the range of 1000 to 1400 ppm, and may depend on how the experiment is carried out, including the analysis of the variation with charge carrier concentration.  $^{38,39,49}$ 

These "experimental" <sup>207</sup>Pb chemical shifts for PbTe, obtained from extrapolation to zero concentration, for the carrier density can be compared with the chemical shift calculated with DFT including relativistic effects through the ZORA that includes scalar and spin—orbit effects. For the lead chemical shifts, the model is a lead atom surrounded by an octahedral array of six tellurium atoms; six hydrogen atoms were included to compensate the major charge on the cluster. For chemical shift referencing, the lead chemical shielding of TML was calculated at the same level of theory. The results in Table 1 indicate that the diamagnetic contribution to the

Table 1. Calculated Lead Chemical Shieldings for  $\left[PbTe_6H_6\right]^{-4}$ 

Pb—Te distance (pm)	$\sigma_{ ext{dia}} ( ext{ppm})$	$\sigma_{ ext{para}} ( ext{ppm})$	$\sigma_{ ext{SO}} ( ext{ppm})$	$\sigma_{ m iso} \ ( m ppm)$	$\delta_{ m iso} \ ( m ppm)$
298	9950	-4960	2867	7857	-513
303	9950	-5182	2830	7599	-256
308	9950	-5463	2785	7273	71
313	9950	-5815	2734	6870	474
318	9950	-6249	2683	6384	959
323	9950	-6794	2636	5793	1550
328	9950	-7442	2606	5114	2229

chemical shielding of lead is virtually independent of the Pb—Te distance, reflecting the major contributions from lead core electrons. This relative constancy of the diamagnetic contribution has also been observed in calculations of the <sup>207</sup>Pb chemical shifts of the lead dihalides and the lead tetrahalides. The paramagnetic and spin—orbit contributions, on the other hand, depend on the Pb—Te bond distance, so that the total chemical shift is dependent on the Pb—Te bond distance, as can be seen by the results in the last column of Table 1. The calculated shift of 1,550 ppm for a PbTe bond length of 323 pm, matching the bond length reported in the crystal structure, <sup>52,53</sup> is in agreement with the shifts observed in the commercial PbTe sample containing native defects and impurities.

For the tellurium resonance, the line shape of the commercial sample is relatively symmetric, as can be seen in Figure 1b, with a mean resonance position of -1176 ppm. The resonance covers a range from roughly -1150 ppm to -1225 ppm. In this case, it is difficult to know the chemical shift by assuming it is at the "edge" of the pattern, but a rough estimate would be around -1150 ppm. The earlier literature, in a study<sup>3</sup> of n- and p-type PbTe as a function of the carrier concentration, indicated a magnetic field of 9689 gauss as the resonance field at 13.0 MHz for the  $^{125}$ Te chemical shift at 77 K. This corresponds to a

chemical shift of -1147 ppm at 77 K. The measured <sup>125</sup>Te shift of -1176 ppm suggests that the sample is a p-type semiconductor, in agreement with the <sup>207</sup>Pb result. According to Balz et al., <sup>54</sup> the shape of <sup>125</sup>Te MAS spectra (e.g., Figure 1b) could be explained using  $J(^{207}\text{Pb}, ^{125}\text{Te}) = 2150$  Hz for various isotopomers of a TePb<sub>6</sub> species to account for the width and shoulders in the spectrum. The chemical shift of the <sup>125</sup>Te resonance has been explained in ref 55.

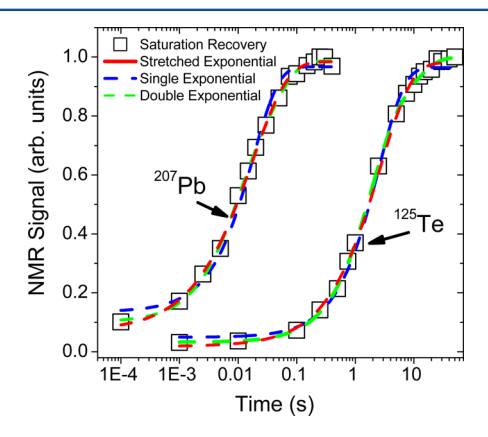
A model to calculate the <sup>125</sup>Te chemical shift is a cluster consisting of a tellurium atom surrounded by an octahedral array of six lead atoms. To terminate the structure, fluorine atoms are appended to the lead atoms. The chemical shift as a function of Pb—Te distance is given in Table 2, reported as the

Table 2. Calculated Tellurium Chemical Shieldings for  $\left[\text{TePb}_6F_{18}\right]^{-8}$ 

$\sigma_{ ext{dia}} \ ( ext{ppm})$	$\sigma_{ ext{para}} \ ( ext{ppm})$	$\sigma_{ ext{SO}} ( ext{ppm})$	$\sigma_{ m iso} \ ( m ppm)$	$\delta_{ m iso} \ ( m ppm)$
5311	-2499	1357	4169	-1070
5311	-2559	1439	4191	-1093
5311	-2628	1529	4212	-1113
5311	-2705	1626	4232	-1134
5311	-2792	1733	4252	-1153
5311	-2891	1846	4266	-1167
	(ppm) 5311 5311 5311 5311 5311	(ppm) (ppm) 5311 -2499 5311 -2559 5311 -2628 5311 -2705 5311 -2792	(ppm)         (ppm)         (ppm)           5311         -2499         1357           5311         -2559         1439           5311         -2628         1529           5311         -2705         1626           5311         -2792         1733	(ppm)         (ppm)         (ppm)         (ppm)           5311         -2499         1357         4169           5311         -2559         1439         4191           5311         -2628         1529         4212           5311         -2705         1626         4232           5311         -2792         1733         4252

shift relative to that of neat dimethyltelluride  $^{11}$  calculated at the same level of theory. The predicted chemical shift changes with the internuclear distance, but not to the extent that the lead chemical shift changes with internuclear distance. Over the same range of bond distance, the lead shift changes roughly five times as rapidly as the tellurium chemical shift. This theoretical observation is consistent with the generally narrower  $^{125}$ Te band as compared to the changes of lead chemical shifts. The predicted  $^{125}$ Te chemical shift is -1134 ppm for the measured bond length. This is in good agreement with the experimentally observed value of -1176 ppm.

**Spin–Lattice Relaxation.** The spin–lattice relaxation time,  $T_1$ , is a useful probe of electronic structure in semiconductors. The  $^{207}\text{Pb}$  and  $^{125}\text{Te}$  spin–lattice relaxation behaviors in saturation-recovery experiments have been measured as a function of temperature. A typical recovery of  $^{207}\text{Pb}$  nuclear longitudinal magnetization at 295 K is shown in Figure 2,



**Figure 2.** <sup>207</sup>Pb and <sup>125</sup>Te saturation recovery of PbTe. The data represent integral intensities of the entire resonance. The dashed line is a fit to a single-exponential (blue) and to a double exponential saturation-recovery model (green). The red line is a fit to a stretched-exponential saturation-recovery model.

together with a stretched exponential function representing the "best fit" to the data. Each data point in the graph of Figure 2 represents the integral of the NMR spectrum across the entire range of frequencies. Therefore, relaxation in regions with different Knight shifts are included, yielding a distribution of relaxation times. The data are not fit by a single exponential as would be expected if all nuclei in the sample recovered with the same rate constant. Figure 3 compares the fully relaxed <sup>207</sup>Pb

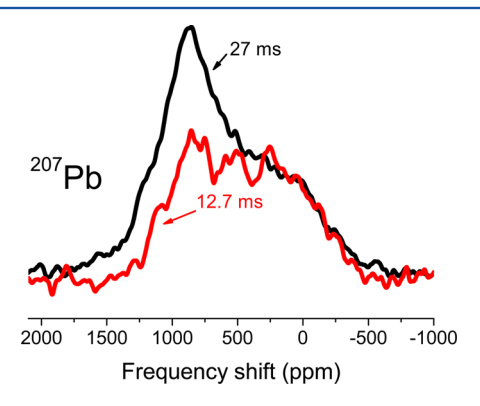


**Figure 3.** Comparison of the <sup>207</sup>Pb spectrum obtained in the saturation-recovery experiment with a delay after saturation of 10 ms (red line) and for a fully relaxed spectrum (black line) of PbTe at 295 K. Relaxation recovery is not uniform across the resonance. The regions at more negative shifts relax more quickly (12.7 ms) than do those at more positive shifts (27 ms, fully relaxed).

spectrum with a partially relaxed spectrum ( $\tau=10~{\rm ms}$ ) of the sample. It is clear from this figure that the relaxation is inhomogeneous, with the regions of the line shape at more negative shifts being relaxed faster than those at less negative shifts. Treating the most intense spectral feature around 875 ppm as a single isochromat yields a  $^{207}{\rm Pb}~T_1$  of approximately 27 ms, while the more rapidly recovering part in the range 700 ppm to  $-500~{\rm ppm}$  has a  $T_1$  around 12.7 ms. As the rate of relaxation,  $1/T_1$ , is known to be proportional to the carrier density,  $^{20,38,48}$  the variation of  $T_1$  across the line shape suggests that the line shape arises from an inhomogeneous distribution of defects, creating domains with differing carrier concentrations. The shorter  $T_1$  and the increased Knight shift to lower frequency are consistent with an increased carrier concentration. This shift to lower frequency of this sample appears to place it in the range of resonances for p-type PbTe semiconductors, as mentioned above.

As a result of the distribution of defects, the <sup>207</sup>Pb spin–lattice relaxation data is best characterized by a Kohlrausch (stretched-exponential) function

$$M(t) = M_0 \left( 1 - \exp\left(-\frac{t}{T_1}\right)^{\beta} \right) \tag{3}$$

The application of this empirical model to physical systems, including NMR relaxation, is well established. It is a natural choice for PbTe, which is characterized by an inhomogeneous distribution of carrier concentrations and defects. The results of this analysis of the  $^{207} \rm Pb$  relaxation rate are shown in Figure 4. The fitting of this plot gives an activation energy of 166 meV (16.02 kJ/mol). This value is virtually identical to the 160 meV (15.4 kJ/mol) activation energy for processes that induce relaxation of  $^{205} \rm Tl$  in semiconducting  $\rm Tl_2 Se.^{57}$ 

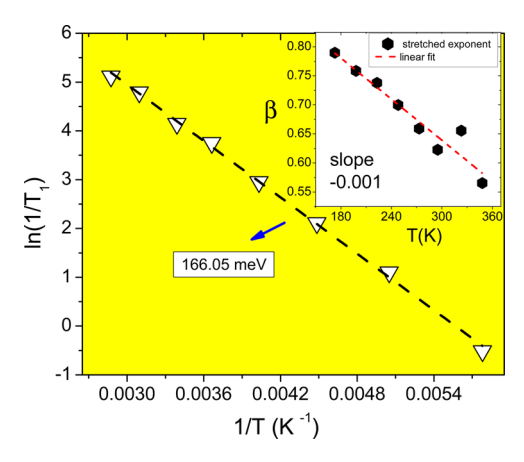


**Figure 4.** (a) The natural logarithm of the average <sup>207</sup>Pb spin—lattice relaxation rate, as a function of the inverse temperature. (b) The exponent  $(\beta)$  obtained from a stretched-exponential fit plotted as a linear function of the temperature.

The  $^{125}$ Te spin—lattice relaxation  $(T_I)$  data from a saturation-recovery experiment at 295 K are shown in Figure 2, as presented next to  $^{207}$ Pb results. As is the case for  $^{207}$ Pb, the relaxation clearly cannot be described as an exponential approach to equilibrium. The result of fitting these data to a stretched exponential function is shown in Figure 5. (For the

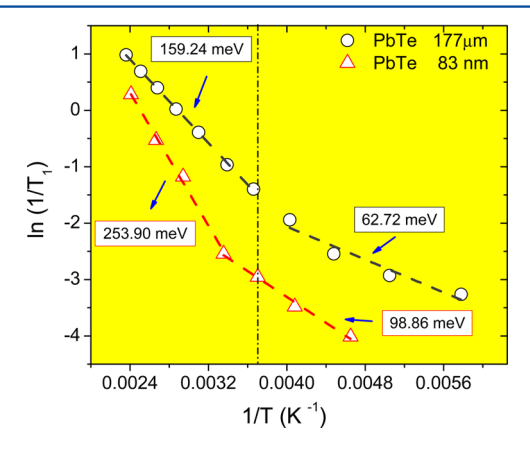


**Figure 5.** The natural logarithm of the  $^{125}$ Te spin—lattice relaxation rate for the case of PbTe (177  $\mu$ m, black open circles) and PbTe (83 nm, red open triangles), as a function of the inverse temperature. Below 250 K, a second mechanism dominates the spin—lattice relaxation in both cases.

interested reader, a biexponential analysis of the same data is provided in the Supporting Information.) In contrast to the results obtained by fitting a stretched-exponential to the 207Pb relaxation data, the 125Te results do not follow Arrhenius behavior with temperature. The low-temperature behavior indicates that, at temperatures below about 250 K, another relaxation mechanism becomes sufficiently effective that it dominates relaxation. The limited data in this region indicate an activation energy of about 62.72 meV for this process. At higher temperatures, a second relaxation mechanism becomes dominant, characterized by an activation energy of 159.24 meV. This second mechanism has, within experimental error, the same activation energy as was observed through the <sup>207</sup>Pb spin-lattice relaxation. It is clear that relaxation of <sup>125</sup>Te in this temperature region and <sup>207</sup>Pb are effected by the same processes, i.e., an interaction with the conduction charge

carriers, but that  $^{125}{\rm Te}$  experiences another mechanism at low temperatures that is not seen to affect the  $^{207}{\rm Pb}$  relaxation.

Temperature-Dependent Changes in Line Shapes. As discussed in the Introduction, there are challenges in accurately determining the "experimental" chemical shift from these earlier studies of PbTe. The challenges include the extrapolation to or estimation of the resonant magnetic field for a sample of zero charge carrier concentration, reading such values from graphs in the literature, and dealing with the effects of temperature upon the shifts. There are also challenges in accurately calculating the chemical shifts of such heavy nuclei that result in significant uncertainty in the predicted chemical shifts. As a result, the assignment of the PbTe used in this study as a p-type semiconductor based on comparisons with the <sup>207</sup>Pb and 125Te "experimental" chemical shifts obtained from the shifts of samples as a function of charge carrier concentration, while strongly suggestive, is still somewhat tenuous. The calculated chemical shifts, also strongly suggestive, do not clearly resolve the issue. The <sup>207</sup>Pb shift of this sample as a function of temperature, shown in Figure 6, exhibits the same

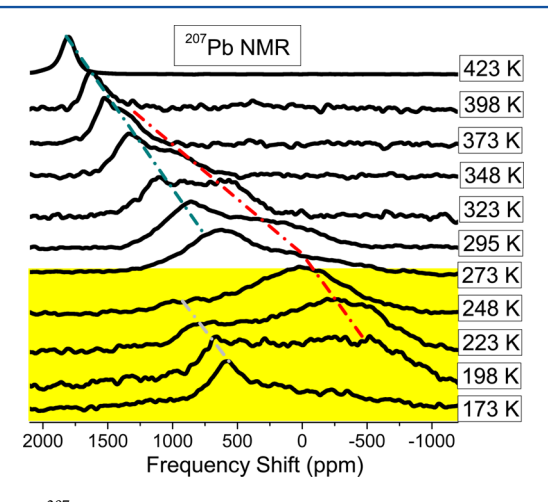


**Figure 6.**  $^{207}\text{Pb}$  NMR spectra of static polycrystalline PbTe from 173 K (bottom) to 423 K (top). The spectrum shape is changing as the temperature increases. Regions with different carrier concentrations shift differently with temperature (as shown by dashed lines). Above 250 K (white regime), the spectrum shifts to higher frequencies accompanied by a reduction in the spread of the spectrum. These two characteristics suggest an annealing of the native defects as the temperature increases.

behavior as that of the p-type samples given in Figure 3 of ref 3. Increasing the temperature of p-type samples of PbTe moves the resonant magnetic field to lower values (corresponding to increases in frequencies at a fixed magnetic field). The opposite behavior is observed for n-type samples. This temperature dependence of the  $^{207}$ Pb shift confirms that the sample used in this study is indeed a p-type semiconductor.

Although the <sup>125</sup>Te chemical shifts at 77 K have been reported as a function of carrier concentration,<sup>3</sup> these early studies of PbTe did not provide any results for the <sup>125</sup>Te chemical shift as a function of temperature for comparison with those obtained in this study. The dependence of the <sup>125</sup>Te shift on temperature for the *p*-type sample of PbTe used in this work is shown in Figure 7. Periodic checks of the sample integrity were made during the variable temperature (VT) studies. This was done by acquiring a one-dimensional <sup>207</sup>Pb spectrum of the sample at 295 K after various stages of the VT study. These

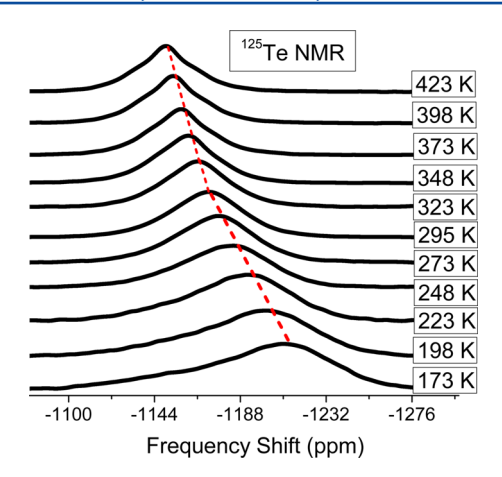


**Figure 7.** <sup>125</sup>Te spectra of static polycrystalline PbTe from 173 K (bottom) to 423 K (top). With increasing temperature, the observed positive shift of spectra is accompanied by a narrowing of the line width and by an alteration of the <sup>125</sup>Te spin—lattice relaxation mechanism.

results are shown in Figure 8. A change in the spectrum appeared after elevating the temperature to 423 K with the

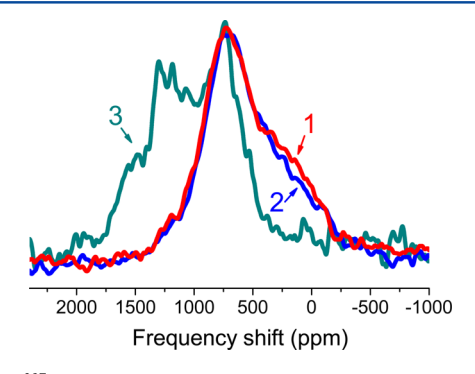


**Figure 8.** <sup>207</sup>Pb spectra of static polycrystalline PbTe acquired at ambient temperature. Spectrum 1 (red line, 1) is prior to any VT experiments. The next spectrum (blue line, 2) is at 295 K after acquiring data at 273 K and then up to and including 398 K. Spectrum 3 (dark cyan line, 3) was acquired at 295 K after first heating the sample to 423 K. No further changes in the ambient temperature <sup>207</sup>Pb spectrum were observed after the saturation-recovery experiments at any of the other lower temperatures.

<sup>207</sup>Pb spectral features moving to a slightly higher NMR frequency. This change is likely due to some annealing of the native defects. The effect is to move the resonance position closer to that of the true chemical shift, as shown in Figure 8. The annealing temperature used in our study is lower than those used in the annealing study of Hewes et al. <sup>58</sup> Due to the high sensitivity of the NMR experiment to sample defects, homogeneity, and carrier concentration (see also ref 57), accuracy in such estimates may require the use of one or more annealing cycles. The lack of sample annealing may lead to systematic errors in the estimation of the chemical shift. In addition to the observed <sup>207</sup>Pb shift, the changes upon annealing will also manifest themselves in the <sup>207</sup>Pb spin—lattice relaxation time.

Another source of systematic errors arises from the powdering of the samples and can alter the NMR shift (and consequently, the spin—lattice relaxation rate). The early NMR studies  $^{2-7}$  of semiconductors usually determined the carrier

concentrations on single crystal specimens and then powdered the samples for the NMR measurements. Hewes et al.<sup>6</sup> noted that the powdering process can alter the carrier concentration. For lead telluride, differences in carrier concentration were noted between those samples cleaved with a razor blade and those crushed with a mortar and pestle. 6,58 The annealing study<sup>58</sup> of *n*- and *p*-type PbTe should generally help in determining error propagation arising from changes in carrier concentration, as carrier concentration as a function of annealing temperature in the range of 452 K and 1000 K are reported. In previous studies on PbTe samples ball milled for 60 min, 59,60 the crystallinity was preserved, but carrier concentration decreased. The decrease in carrier concentration in nanocrystalline samples is referred as the "self-cleaning" process of the bulk,  $^{61-64}$  whereby defects are pushed toward the surface. The nanoparticles possess fewer defects than the corresponding bulk material. Because of self-cleaning in nanoparticles, ball-milling would be expected to decrease the spin-lattice relaxation rate  $(1/T_1)$ , as shown in Figure 5 for the finest ball-milled PbTe (83 nm). The self-cleaning process is directly related to the observed increase in the activation energy in the high and low temperature regime (<250 K). In Figure 9,

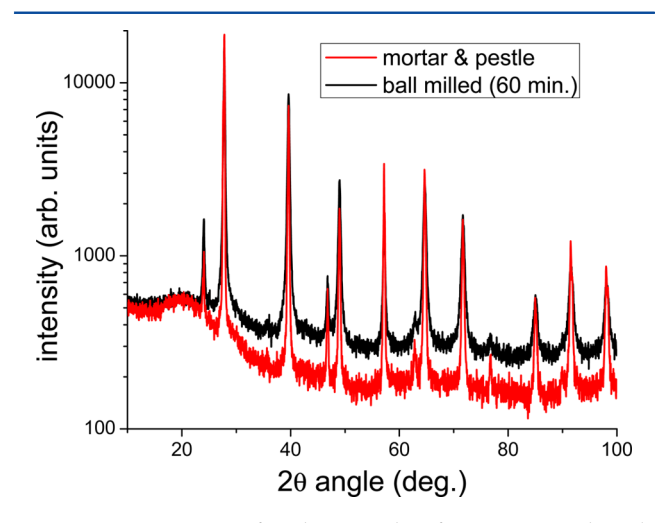


**Figure 9.** PXRD spectra for PbTe powders from mortar and pestle versus ball-milled processes confirm that the samples preserve their crystallinity. For the ball-milled (60 min) sample, the average particle size was estimated from the PXRD data to be 83 nm, using the Scherer formula.

powder X-ray diffraction (PXRD) spectra for powdered PbTe ingots (Alfa Aesar, Ward Hill, MA) mortar and pestle versus bal- milled (83 nm, 60 min ball milling) samples confirm that crystallinity is indeed preserved. However, the carrier concentration in these samples appears to change, as evidenced by the increased  $T_1$  time with decreasing particle size (Table 3).

Atomic self-diffusion of Pb and Te has been investigated<sup>65</sup> in lead telluride at temperatures in the range 793–1000 K with use of radioactive tracers. The self-diffusion coefficients reported were quite high:  $2.9 \times 10^{-5}$  cm<sup>2</sup>/sec for Pb and  $2.7 \times 10^{-6}$  cm<sup>2</sup>/s for Te. While the activation energy for diffusion of Pb was dependent upon the stoichiometry of the sample, the lowest measured activation for both Pb and Te at 100 kJ/mol is still much higher than the activation energies found in the current investigation. Thus, the relaxation mechanism in the high-temperature regime cannot be due to atomic diffusion. The likely mechanism involves interactions of nuclear moments

Table 3. Comparison of  $T_1$  Relaxation Times for Lead Telluride Ball Milled for Various Times<sup>a</sup>

vendor	powdering method	milling time	average nanocrystal size	$T_1$	Kohlrausch exponent $(\beta)$
Sigma- Aldrich	used as-is (mesh140)	n/a	n/a	2.6 s	0.80
Alfa Aesar	mortar and pestle	n/a	n/a	6.8 s	0.44
Alfa Aesar	ball milled	1 min	326 nm	6.7 s	0.53
Alfa Aesar	ball milled	5 min	151 nm	12.7 s	0.55
Alfa Aesar	ball milled	15 min	131 nm	12.7 s	0.55
Alfa Aesar	ball milled	30 min	98 nm	12.7 s	0.55
Alfa Aesar	ball milled	60 min	83 nm	12.7 s	0.55

<sup>a</sup>The average particle size of nanocrystalline powders was estimated from PXRD data using the Scherrer formula.

with thermally activated charge carriers. 46,47,57 The low-temperature process that affects the <sup>125</sup>Te relaxation can be, like for TlTaS<sub>3</sub>, due to spin diffusion to localized electron spins.

MAS does not lead to a significant narrowing of the <sup>207</sup>Pb resonance, as shown in Figure 1a. The shift to higher frequency is consistent with an increased temperature in the MAS rotor resulting from the sample spinning at 10 kHz. <sup>38,41,66</sup> A measurement of the <sup>207</sup>Pb NMR shift of lead nitrate <sup>12–19</sup> at an ambient temperature of 295 K indicates a sample temperature of 306 K at this rotation rate. However, the magnitude of the change in the shift at 140 ppm for the MAS spectrum is much larger than that expected from frictional heating of the MAS rotor alone. Such an effect of similarly large shifts in MAS spectra of conductive samples has been explained <sup>66</sup> for spectra of CuI. This shift to higher frequency for the <sup>207</sup>Pb resonance of a static sample of lead telluride as the temperature is increased is demonstrated in Figure 6. MAS increases the magnitude of this shift in conductive samples.

MAS also does not substantially narrow the <sup>125</sup>Te resonance, as shown in Figure 1b. The rotation rate of 10 kHz is larger than the <sup>125</sup>Te static line width of 4.7 kHz. As MAS does not result in a manifold of spinning sidebands in either the <sup>207</sup>Pb or <sup>125</sup>Te MAS spectra, the broadening of the spectral resonance is not due solely to an orientational dependence of chemical shifts (or Knight shifts). While Figure 7 shows that the <sup>125</sup>Te resonance of the static sample exhibits the same shift to increasing frequency as the temperature is raised as observed with the <sup>207</sup>Pb spectra shown in Figure 6, the <sup>125</sup>Te MAS spectrum in Figure 1b shows a slight narrowing of the resonance with a shift of the first moment of the resonance to lower frequency. This likely arises due to the averaging of anisotropic interactions.

#### CONCLUSIONS

Unless samples of zero Knight shift (i.e., with low carrier concentration) are available as a reference, the chemical and Knight shifts are normally distinguished through detailed studies of the resonance frequency as a function of temperature and carrier concentration, followed by extrapolation of the shift to zero carrier concentration. In order to overcome this time-consuming approach, we present here combined NMR and DFT methods to separate these two contributions. A second

advantage of the approach is that it enables studies of specific samples with fixed physical properties whose carrier concentrations cannot easily be altered. Calculations of the chemical shift of PbTe based on model structures are in agreement with experiment. Experiments confirm that PbTe consists of a distribution of crystallites having differing densities of charge carriers, resulting in an asymmetric line shape due to a distribution of Knight shifts in various domains of the sample. Our results suggest that the sample studied was *p*-type, in agreement with previous carrier concentration-dependent studies of *n*- and *p*-type PbTe semiconductor.

Relaxation studies show that the sample exhibits dynamics that arise from a range of charge carrier densities. In the high-temperature regime, relaxation is governed by interaction with thermally activated charge carriers. For <sup>125</sup>Te at temperatures below about 250 K, a second mechanism dominates spin—lattice relaxation, which we postulate may be due to spin diffusion to isolated electron spins. The low temperature regime is also suggestive that a second mechanism affects <sup>207</sup>Pb relaxation. Thus, interaction with both mobile carriers and fixed centers contributes to relaxation in PbTe.

The literature data on PbTe have been converted to the currently accepted shift scale. We also provide possible evidence for the "self-cleaning effect" property of PbTe nanocrystals whereby defects are removed from the core of the particles while preserving the crystal structure.

## ASSOCIATED CONTENT

# Supporting Information

Conversion of shift measurements and <sup>125</sup>Te NMR analysis by double exponential model. This material is available free of charge via the Internet at http://pubs.acs.org.

#### AUTHOR INFORMATION

# **Corresponding Author**

\*E-mail: bouchard@chem.ucla.edu.

#### Notes

The authors declare no competing financial interest.

#### ACKNOWLEDGMENTS

This material is based upon work supported by the National Science Foundation through Grant CHEM0956006 to C.D. The work at UCLA (L.-S.B.) was supported by the Defense Advanced Research Project Agency (DARPA), Award No. N66001-12-1-4034. L.-S.B. acknowledges useful discussions with Mercouri G. Kanatzidis.

## REFERENCES

- (1) LaLonde, A. D.; Pei, Y.; Wang, H.; Snyder, G. J. Lead Telluride Alloy Thermoelectrics. *Mater. Today* **2011**, *14*, 526–532.
- (2) Sapoval, B. Knight Shifts and Band Structure in Lead Telluride by Helicon-Nuclear-Spin Interaction. *J. Phys. (Paris), Suppl.* **1968**, 29, C4-133–C4-136.
- (3) Senturia, S. D.; Smith, A. C; Hewes, C. R.; Hofmann, J. A.; Sagalyn, P. S. Knight Shfits and Band Structure in the Lead–Salt Semiconductors. *Phys. Rev. B* **1970**, *1*, 4045–4057.
- (4) Sapoval, B.; Leloup, J. Y. Knight Shift in Multivalley Semiconductors. I. Theory of Contact, Orbital, and Dipolar Shift and Relativistic Effects. *Phys. Rev. B* **1973**, *7*, 5272–5276.
- (5) Leloup, J. Y.; Sapoval, B.; Martinez, G. Knight Shift in Multivalley Semiconductors. II. Determination of the Hyperfine Coupling Constants in *n* and *p*-Type PbSe and PbTe. *Phys. Rev. B* **1973**, *7*, 5276–5284.

- (6) Hewes, C. R.; Adler, M. S.; Senturia, S. D. Nuclear-Magnetic-Resonance Studies in PbTe and  $Pb_{1-x}Sn_xTe$ : An Experimental Determination of  $\vec{k}\cdot\vec{p}$  Band Parameters and Magnetic Hyperfine Constants. *Phys. Rev. B* **1973**, *7*, 5195–5211.
- (7) Martinez, G.; Schlüter, M.; Cohen, M. L. Electronic structure of PbSe and PbTe. I. Band Structures, Densities of States, and Effective Masses. *Phys. Rev. B* **1975**, *11*, 651–659.
- (8) Knight, W. D. Nuclear Magnetic Resonance Shift in Metals. *Phys. Rev.* **1949**, *76*, 1259–1260.
- (9) Proctor, W. G.; Yu, F. C. The Dependence of a Nuclear Magnetic Resonance Frequency upon Chemical Compound. *Phys. Rev.* **1950**, *77*, 717–717.
- (10) Dickenson, W. C. Dependence of the F19 Nuclear Resonance Position on Chemical Compound. *Phys. Rev.* **1950**, *77*, 736–737.
- (11) Harris, R. K.; Becker, E. D.; Cabral de Menezes, S. M.; Goodfellow, R.; Granger, P. NMR Nomenclature. Nuclear Spin Properties and Conventions for Chemical Shifts. *Pure Appl. Chem.* **2001**, 73, 1795–1818.
- (12) Bielecki, A.; Burum, D. P. Temperature Dependence of <sup>207</sup>Pb MAS Spectra of Solid Lead Nitrate. An Accurate, Sensitive Thermometer for Variable-Temperature MAS. *J. Magn. Reson. A* **1995**, *116*, 215–220.
- (13) Ferguson, D. B.; Haw, J. F. Transient Methods for in Situ NMR of Reactions on Solid Catalysts Using Temperature Jumps. *Anal. Chem.* **1995**, *67*, 3342–3348.
- (14) van Gorkom, L. C. M.; Hook, J. M.; Logan, M. B.; Hann, J. V.; Wasylishen, R. E. Solid-State Lead-207 NMR of Lead(II) Nitrate: Localized Heating Effects at High Magic Angle Spinning Speeds. *Magn. Reson. Chem.* **1995**, 33, 791–795.
- (15) Mildner, T.; Ernst, H.; Freude, D. <sup>207</sup>Pb NMR Detection of Spinning-Induced Temperature Gradients in MAS Rotors. *Solid State NMR* 1995, *5*, 269–271.
- (16) Neue, G.; Dybowski, C. Determining Temperature in a Magic-Angle Spinning Probe Using the Temperature Dependence of the Isotropic Chemical Shift of Lead Nitrate. *Solid State NMR* **1997**, *7*, 333–336.
- (17) Takahashi, T.; Kawashima, H.; Sugisawa, H.; Baba, T. <sup>207</sup>Pb Chemical Shift Thermometer at High Temperature for Magic Angle Spinning Experiments. *Solid State NMR* **1999**, *15*, 119–123.
- (18) Beckmann, P. A.; Dybowski, C. A Thermometer for Nonspinning Solid-State NMR Spectroscopy. *J. Magn. Reson.* **2000**, 146, 379–380.
- (19) Dybowski, C.; Neue, G. Solid-State <sup>207</sup>Pb NMR Spectroscopy. Prog. Nucl. Magn. Reson. Spectrosc. **2002**, 41, 153–170.
- (20) Levin, E. M.; Cook, B. A.; Ahn, K.; Kanatzidis, M. G.; Schmidt-Rohr, K. Electronic Inhomogeneity and Ag:Sb Imbalance of Ag<sub>1-y</sub>Pb<sub>18</sub>Sb<sub>1+z</sub>Te<sub>20</sub> High-Performance Thermoelectrics Elucidated by <sup>125</sup>Te and <sup>207</sup>Pb NMR. *Phys. Rev. B* **2009**, *80*, 115211.
- (21) Andrew, E. R.; Bradbury, A.; Eades, R. G. Nuclear Magnetic Resonance Spectra from a Crystal Rotated at High Speed. *Nature* **1958**, *182*, 1659.
- (22) Andrew, E. R.; Bradbury, A.; Eades, R. G. Removal of Dipolar Broadening of Nuclear Magnetic Resonance Spectra of Solids by Specimen Rotation. *Nature* **1959**, *183*, 1802–1803.
- (23) Lowe, I. J. Free Induction Decays of Rotating Solids. *Phys. Rev. Lett.* **1959**, *2*, 285–287.
- (24) Farrar, T. C.; Becker, E. D. Pulse and Fourier Transform NMR, Introduction to Theory and Methods; Academic Press: New York, 1971.
- (25) Collins, M. J.; Ripmeester, J. A.; Sawyer, J. F. CP/MAS <sup>125</sup>Te NMR in Solids: An Example of <sup>125</sup>Te-<sup>35,37</sup>Cl *J* Couplings. *J. Am. Chem. Soc.* **1987**, *109*, 4113–4115.
- (26) Jameson, C. J.; Jameson, A. K. Concurrent <sup>19</sup>F and <sup>77</sup>Se or <sup>19</sup>F and <sup>125</sup>Te NMR  $T_I$  Measurements for Determination of <sup>77</sup>Se and <sup>125</sup>Te Absolute Shielding Scales. *Chem. Phys. Lett.* **1987**, *135*, 254–259.
- (27) Ruiz-Morales, Y.; Schreckenbach, G.; Ziegler, T. Calculation of <sup>125</sup>Te Chemical Shifts Using Gauge-Including Atomic Orbitals and Density Functional Theory. *J. Phys. Chem. A* **1997**, *101* (2), 4121–4127.

- (28) Fukuda, R.; Nakatsuji, H. Quasirelativistic Theory for the Magnetic Shielding Constant. III. Quasirelativistic Second-Order Møller—Plesset Perturbation Theory and Its Application to Tellurium Compounds. *J. Chem. Phys.* **2005**, *123*, 044101.
- (29) Baerends, E. J.; Ziegler, T.; Autschbach, J.; Bashford, D.; Bérces, A.; Bickelhaupt, F. M.; Bo, C.; Boerrigter, P. M.; Cavallo, L.; Chong, D. P.; et al. *ADF2012, SCM*; Theoretical Chemistry, Vrije Universiteit: Amsterdam, The Netherlands, 2012 (http://www.scm.com).
- (30) Guerra, C. F.; Snijders, J. G.; te Velde, G.; Baerends, E. J. Towards an order-N DFT method. *Theor. Chem. Acc.* **1998**, 99 (6), 391–403.
- (31) te Velde, G.; Bickelhaupt, F. M.; Baerends, E. J.; Guerra, C. F.; Van Gisbergen, S. J. A.; Snijders, J. G.; Ziegler, T. Chemistry with ADF. *J. Comput. Chem.* **2001**, 22 (9), 931–967.
- (32) Becke, A. D. Density-Functional Exchange-Energy Approximation with Correct Asymptotic Behavior. *Phys. Rev. A* **1988**, 38, 3098–3100.
- (33) Perdew, J. P. Density-Functional Approximation for the Correlation Energy of the Inhomogeneous Electron Gas. *Phys. Rev.* B 1986, 33, 8822–8824.
- (34) van Lenthe, E.; Baerends, E. J.; Snijders, J. G. Relativistic Regular Two-Component Hamiltonians. *J. Chem. Phys.* **1993**, *99*, 4597–4610.
- (35) van Lenthe, E.; Ehlers, A.; Baerends, E. J. Geometry Optimizations in the Zero Order Regular Approximation for Relativistic Effects. *J. Chem. Phys.* **1999**, *110*, 8943–8953.
- (36) Schreckenbach, G.; Ziegler, T. Calculation of NMR Shielding Tensors Using Gauge-Including Atomic Orbitals and Modern Density Functional Theory. *J. Phys. Chem.* **1995**, *99*, 606–611.
- (37) Brevard, C.; Granger, P. Handbook of High Resolution Multinuclear NMR; John Wiley and Sons: New York, 1981.
- (38) Yesinowski, J. P.; Purdy, A. P.; Wu, H.; Spencer, M. G.; Hunting, J.; DiSalvo, F. J. Distributions of Conduction Electrons as Manifested in MAS NMR of Gallium Nitride. *J. Am. Chem. Soc.* **2006**, 128 (15), 4952–4953.
- (39) Holloway, H. Growth and Application of Epitaxial IV-VI Compounds. J. Nonmet. 1973, 1, 347-354.
- (40) Yesinowski, J. P. <sup>69,71</sup>Ga and <sup>14</sup>N High-Field NMR of Gallium Nitride Films. *Phys. Status Solidi* **2005**, 2 (7), 2399–2402.
- (41) Yesinowski, J. P. Solid-State NMR of Inorganic Semiconductors. *Top. Curr. Chem.* **2012**, 306, 229–312.
- (42) Hirsch, M. J.; Holcomb, D. F. NMR Study of Si:As and Si:P near the Metal-Insulator Transition. *Phys. Rev. B* **1986**, 33, 2520–2529.
- (43) Tripathi, G. S.; Das, L. K.; Misra, P. K.; Mahanti, S. D. Spin-Orbit Effects on Knight Shift A New Contribution. *Solid State Commun.* **1981**, 38, 1207–1210.
- (44) Misra, S.; Tripathi, G. S.; Misra, P. K. Theory of the Knight Shift in Narrow-Gap Semiconductor. *J. Phys. C: Solid State Phys.* **1987**, 20, 277.
- (45) Misra, C. M.; Tripathi, G. S. Knight Shift in PbTe AND Pb1-xSnxTe. Hyperfine Interact. 1990, 60, 619–622.
- (46) Koumoulis, D.; Chasapis, T. C.; Taylor, R. E.; Lake, M. P.; King, D.; Jarenwattananon, N. N.; Fiete, G. A.; Kanatzidis, M. G.; Bouchard, L. S. NMR Probe of Metallic States in Nanoscale Topological Insulators. *Phys. Rev. Lett.* **2013**, *110*, 026602.
- (47) Taylor, R. E.; Leung, B.; Lake, M. P.; Bouchard, L. S. Spin-Lattice Relaxation in Bismuth Chalcogenides. *J. Phys. Chem. C* 2012, 116 (32), 17300–17305.
- (48) Alexander, M. N.; Sagalyn, P. L.; Senturia, S. D.; Hewes, C. R. Nuclear Spin Relaxation Study of the Electronic Structure of Lead Telluride. *J. Nonmet.* 1973, 1, 251.
- (49) Olekseeva, M. F.; Slinko, E. I.; Tovstyuk, K. D.; Handozhko, A. G. Nuclear Magnetic Resonance in PbTe. *Phys. Status Solidi* **1974**, *21* (A), 759–762.
- (50) Yafet, Y.; Jaccarino, V. Nuclear Spin Relaxation in Transition Metals; Core Polarization. *Phys. Rev.* **1964**, *133*, A1630–A1637.
- (51) Dmitrenko, O.; Bai, S.; Dybowski, C. Prediction of <sup>207</sup>Pb NMR Parameters for the Solid Ionic Lead (II) Halides Using the Relativistic

- ZORA-DFT Formalism: Comparison with the Lead-Containing Molecular Systems. Solid State Nucl. Magn. Reson. 2008, 34, 186–190.
- (52) Noda, Y.; Ohba, S.; Sato, S.; Saito, Y. Charge Distribution and Atomic Thermal Vibration in Lead Chalcogenide Crystals. *Acta Crystallogr., Sect B: Struct. Sci.* 1983, 39, 312–317.
- (53) Noda, Y.; Masumoto, K.; Ohba, S.; Saito, Y.; Toriumi, Y. K.; Iwata, Y.; Shibuya, I. Temperature Dependence of Atomic Thermal Parameters of Lead Chalcogenides, PbS, PbSe, and PbTe. *Acta Crystallogr., Sect. C: Cryst. Struct. Commun.* 1987, 43, 1443–1445.
- (\$4) Balz, R.; Haller, M.; Hertler, W. E.; Lutz, O.; Nolle, A.; Schafitel, R. <sup>125</sup>Te NMR Studies of Indirect and Direct Dipole—Dipole Coupling in Polycrystalline CdTe, HgTe, and PbTe. *J. Magn. Reson.* **1980**, *40*, 9–16.
- (55) Koch, W.; Lutz, O.; Nolle, A. <sup>77</sup>Se and <sup>125</sup>Te Nuclear Magnetic Resonance Investigations in II–VI and IV–VI Compounds. *Z. Phys. A: Hadrons and Nuclei* **1978**, 289, 17–20.
- (56) Beckmann, P. A.; Schneider, E. Methyl Group Rotation, <sup>1</sup>H Spin-Lattice Relaxation in an Organic Solid, and the Analysis of Non-exponential Relaxation. *J. Chem. Phys.* **2012**, *136*, 054508.
- (57) Panich, A. M.; Shao, M.; Teske, C. L.; Bensch, W. Size-Dependent Properties of Tl<sub>2</sub>Se Studied by NMR Spectroscopy. *Phys. Rev. B* **2006**, *74*, 233305.
- (58) Hewes, C. R.; Adler, M. S.; Senturia, S. D. Annealing Studies of PbTe and  $Pb_{1-x}Sn_xTe$ . *J. Appl. Phys.* **1973**, *44*, 1327–1332.
- (59) Lim, P. N. et al. Synthesis and processing of nanostructured thermoelectric materials. In *SIMTech Technical Reports* (STR V12 N3 01 FTG); Vol. 12 Number 3, 2011.
- (60) Bouad, N.; Marin-Ayral, R. M.; Tedenac, J. C. Mechanical Alloying and Sintering of Lead Telluride. *J. Alloys Compd.* **2000**, 297 (1–2), 312–318.
- (61) Martin, J.; Nolas, G. S.; Zhang, W.; Chen, L. PbTe Nanocomposites Synthesized from PbTe Nanocrystals. *Appl. Phys. Lett.* **2007**, *90*, 222112–222112–3.
- (62) Oh, T. S.; Choi, J.; Hyun, D. B. Formation of PbTe Intermetallic Compound by Mechanical Alloying of Elemental Pb and Te Powders. *Scr. Metall. Mater.* **1995**, 32 (4), 595–600.
- (63) Bouad, N.; Marin-Ayral, R. M.; Tedenac, J. S. Mechanical Alloying and Sintering of Lead Telluride. *J. Alloys Compd.* **2000**, 297, 312–318.
- (64) Lee, H. E.; Lee, D. Y.; Kim, I. J.; Woo, B. C. Manufacturing and Characterization of Nano-Sized PbTe Powders. *Proceedings ICT '02. Twenty-First International Conference on Thermoelectrics, 2002*; IEEE: Piscataway, NJ, 2002.
- (65) Gomez, M. P.; Stevenson, D. A.; Huggins, R. A. Self-Diffusion of Pb and Te in Lead Telluride. *J. Phys. Chem. Solids* **1971**, *32*, 335–344. (66) Yesinowski, J. P.; Ladouceur, H. D.; Purdy, A. P.; Miller, J. B.
- (66) Yesinowski, J. P.; Ladouceur, H. D.; Purdy, A. P.; Miller, J. B. Electrical and Ionic Conductivity Effects on Magic-Angle Spinning Nuclear Magnetic Resonance Parameters of Cul. *J. Chem. Phys.* **2010**, 133, 234509.